

Structure of the $\text{TiO}_{2-x}(\text{100})-1 \times 3$ surface by direct methods

E. Landree^{a,*}, L.D. Marks^a, P. Zschack^b, C.J. Gilmore^c

^a *Department of Materials Science and Engineering, Northwestern University, Evanston, IL 60208, USA*

^b *Materials Research Laboratory, University of Illinois at Urbana-Champaign, Urbana, IL 61801, USA*

^c *Department of Chemistry, University of Glasgow, Glasgow, G12 8QQ, UK*

Received 18 March 1997; accepted for publication 3 March 1998

Abstract

An improved atomic model of the $\text{TiO}_{2-x}(\text{100})-1 \times 3$ surface has been determined based on grazing incidence X-ray diffraction (GIXD) data analyzed by direct methods coupled with χ^2 minimization. The structure contains edge- and face-sharing octahedra, similar to known defect structures in $\text{Ti}_n\text{O}_{2n-1}$. The final structure consists of four Ti atoms and six to eight oxygen. © 1998 Elsevier Science B.V. All rights reserved.

Keywords: Computer simulations; Direct methods; X-ray scattering, diffraction and reflection; Surface relaxation and reconstruction; $\text{TiO}_{2-x}(\text{100})-1 \times 3$; Titanium oxide; Low index single crystal surfaces

1. Introduction

Studies of the surface of TiO_{2-x} (rutile) have largely been motivated by its catalytic properties for decomposing water into hydrogen and oxygen discovered in the 1970s [1–3]. Since this discovery there have been numerous experimental [4–10] and theoretical [11,12] investigations of the $\text{TiO}_{2-x}(\text{110})$ and $\text{TiO}_{2-x}(\text{100})$ surfaces. Previous studies of the $\text{TiO}_{2-x}(\text{110})-1 \times 1$ surface have revealed that it is quite stable, reconstructing to a 1×2 unit cell only after extended annealing at or above 888 K [5,9]. Unlike the (110) surface, $\text{TiO}_{2-x}(\text{100})$ is capable of forming several different reconstructions, including a 1×3 unit cell when annealed at 873 K. Additional heat treatments at 1073 K and 1473 K yield a 1×5 and 1×7 unit

cell, respectively. A previous study using grazing incidence X-ray diffraction (GIXD) and low energy electron diffraction (LEED) proposed a model for the $\text{TiO}_{2-x}(\text{100})-1 \times 3$ surface consisting of microfaceted $\text{TiO}_{2-x}(\text{110})$ planes based on Patterson functions [10].

A fundamental problem with the microfaceted model, as in many surface structure determinations, is whether something similar to the true structure was used as the source of the initial atomic positions for a refinement. Given any starting set of atomic positions, it is possible to minimize these parameters relative to an experimentally measured set of reflections (LEED, GIXD or transmission electron diffraction) to arrive at a solution. One may find an atomic arrangement that is somewhat consistent with the diffraction intensities, but not the best configuration, thus finding a local minimum rather than a true global minimum. In the initial study [10], Patterson maps

* Corresponding author. Fax: (+1) 847 491 7820;
e-mail: e-landree@nwu.edu

Table 1
Measured k , l , intensity and error in standard crystallographic notation

k	l	$(F_{0kl})^2$	σ
4	0	5.51	3.03
5	0	38.0	2.80
7	0	11.22	2.21
8	0	1.32	1.43
10	0	4.64	3.04
11	0	2.97	2.77
13	0	0.0	1.00
14	0	0.0	1.00
2	1	7.73	4.10
4	1	6.36	3.38
5	1	6.55	3.11
7	1	4.59	1.64
8	1	30.07	1.35
10	1	2.31	0.96
11	1	5.10	1.65
7	2	2.43	2.23
10	2	2.91	1.01
11	2	5.32	2.18
14	2	0.0	1.00

were used to arrive at a starting set of atomic positions that were refined relative to the 19 reflections measured by GIXD. Since Patterson functions only show interatomic vectors, not the true atomic positions, it is difficult to perform a comprehensive search of all possible atomic arrangements, particularly in the case of large unit cell structures.

For the problem of solving bulk crystal structures, a technique known as “direct methods” is now routinely applied. While the literature on

these in the bulk is very extensive [13], it is only very recently that they have been successfully applied to surface diffraction data from either X-rays or high energy electrons [14–20]. A few words of explanation of their basis are appropriate; more details for bulk [13] and for surfaces [14–20] can be found elsewhere. The GIXD experiment yields structure factor moduli from the measured reflections (here 19), and if we can find the corresponding phases the charge density can be reconstructed by a simple Fourier transform. We do not need these phases exactly, only approximate values, to produce a map representative of the charge density. While the number of possible phase choices is exceedingly large, only a few combinations at most need to be considered in any detail. This is because diffraction takes place from atoms which are small, positive sites for the charge density in real space. As a consequence, certain phase relationships [13] connect the phases of the diffracted beams, equivalent to a set of self-consistent equations which have to be satisfied. A search of the possible phases is conducted using one of a number of techniques, e.g. magic-integers [21], random numbers [22], error correcting codes [23] or a genetic algorithm [15,24–26] in a multi-solution approach. These solutions provide a set of plausible phases ranked according to figures of merit (FOMs). The initial charge density maps are generated using these phases and are examined in the order suggested by the FOMs. The charge density maps are used as starting models of the

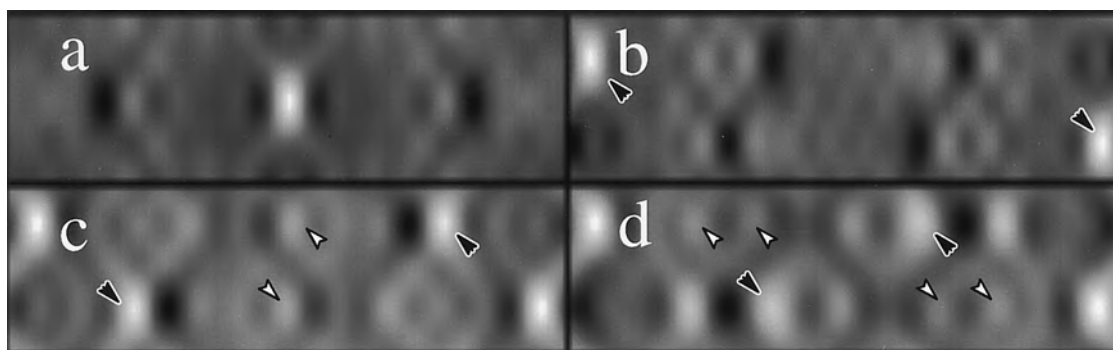


Fig. 1. Charge density maps containing (a) one, (b) two, (c) four, and (d) six atoms in a 1×3 unit cell constructed using the same reflections as those measured experimentally. The positions of the actual atoms within the unit cell have been marked with black arrows for reference, artifact spots have been marked with white arrows.

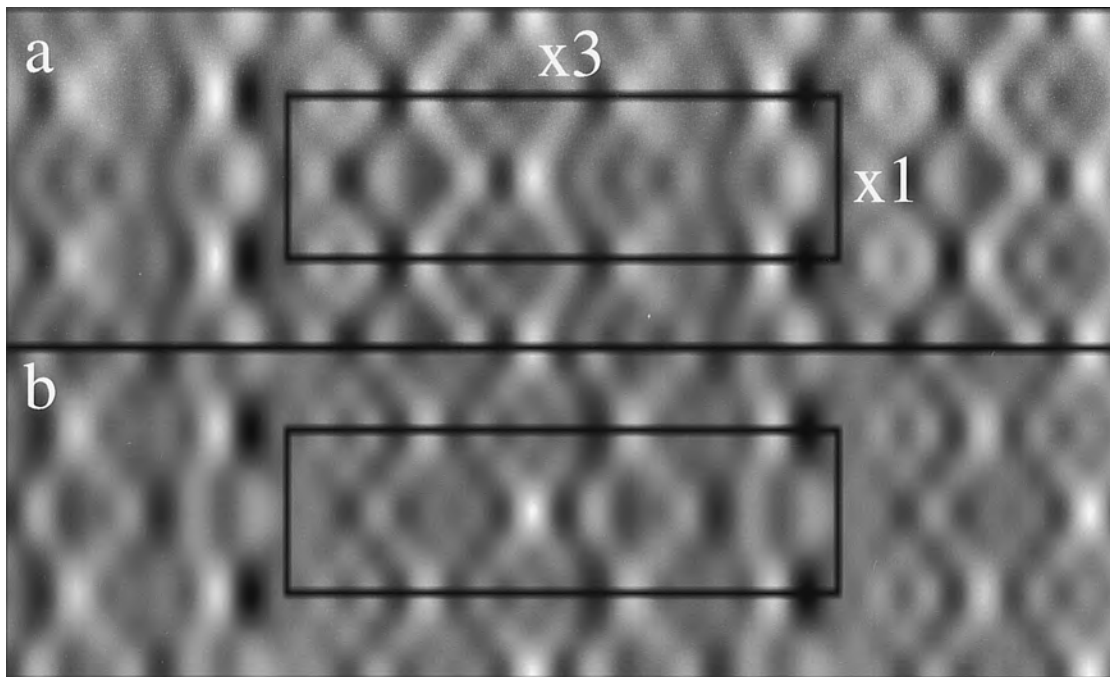


Fig. 2. (a) A charge density map calculated from the direct phasing algorithm. (b) The model constructed by placing single titanium atoms in the unit cell based upon positions indicated in (a).

Table 2

Relative titanium atom positions of $\text{TiO}_{2-x}(100)\text{-}1 \times 3$ models with calculated χ^2 value. The model with four Ti atoms is the best fit to the experimentally measured structure factors

	Relative bulk TiO_{2-x} positions		Micro-facet ^b $p2mm$	Micro-facet pm	Missing row ^b $p2mm$	Missing row pm	4 Ti pm	5 Ti (a)	5 Ti (b)
	x pos	y pos ^a	x pos	x pos	x pos	x pos	x pos	x pos	x pos
Ti 1	0.0	0.0	0.0	0.0	0.0	0.0	0.0	0.0	0.0
Ti 2	0.333	0.0	0.334	0.328	0.340	0.325	0.359	0.139	0.216
Ti 3	0.666	0.0	0.666	0.655	0.660	0.673	0.608	0.782	0.863
Ti 4	0.166	0.5	0.181	0.179	0.173	0.175	0.179	0.184	
Ti 5	0.500	0.5						0.448	0.412
Ti 6	0.833	0.5	0.819	0.812	0.827	0.809			0.535
χ^2			7.83	8.47	9.46	8.87	3.45	5.48	6.41
D.o.F. ^c			15	15	15	15	15	15	15
% ^d			$<10^{-6}$	$<10^{-6}$	$<10^{-6}$	$<10^{-6}$	0.002	$<10^{-6}$	$<10^{-6}$

^a For the pm and $p2mm$ space groups, atomic positions were refined only along the x direction.

^b The microfacet model had two atoms at the origin, modeled by a double occupancy for the purpose of χ^2 refinement.

^c Degrees of freedom: correspond to the number of beams minus the number of fitting parameters.

^d This is the calculated probability in per cent of that value of χ^2 or higher occurring for 1×10^6 repeated experiments. In cases where the χ^2 term is less than 1.0, the value is taken to be the probability of χ^2 or lower occurring. For a model with infinite degrees of freedom (i.e. infinite reflections) with no errors in the measured reflections, the correct solution would have a χ^2 value of 1 or higher 100% of the time for an infinite number of repeated experiments.

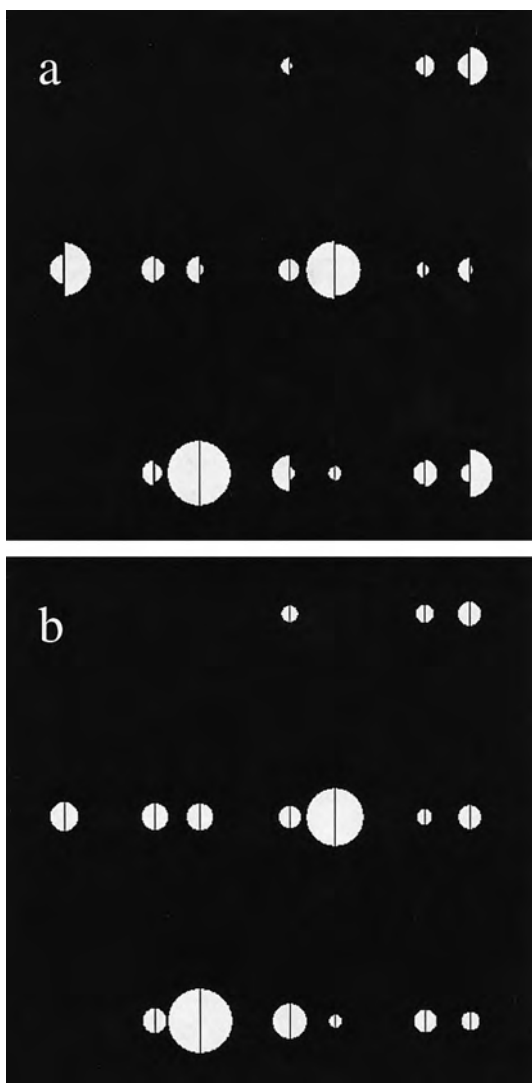


Fig. 3. A schematic of the diffraction pattern containing the 16 measured non-zero values for (a) the microfacet model [10] and (b) the four Ti atom model. The radii of the left semi-circles are proportional to the structure factor of the measured beams, and the radii of the right semi-circles are proportional to the structure factors calculated from the model.

atomic structure that are refined by comparing the observed and calculated crystallographic structure factors, producing a set of refined atomic positions.

In effect the method does a global search finding all atomic arrangements which are consistent with atomic scattering with no initial information other than the diffracted beam intensities and the under-

lying assumptions of direct methods. This technique is routine for X-ray bulk crystal structure determination and is now also being applied to determine the structure of surfaces. As a means of validating the use of this approach, this method has already been applied to several previously known structures, including two-dimensional structure models [15], the Au on Si(111)- $\sqrt{3} \times \sqrt{3}$ and 5×2 [16], and the Si(111)- 7×7 [14]. In each case direct methods successfully found the correct surface structure. The first case where it was applied to an unknown structure was the In on Si(111)- 4×1 surface [18]. Application of direct methods to the TiO_{2-x} (100)- 1×3 surface is the second case where it has been applied to an unknown structure and the first for an unknown native reconstruction. It has subsequently been used for the Au on Si(111)- 6×6 [19], Ag on Si(111)- 3×1 [20] and for two three-dimensional cases. We find a much better model for the surface than the previously proposed microfacet model [10].

2. Method

The magnitudes of the structure factors for the 19 measured beams are listed in Table 1. The original source of this table and a detailed explanation of how the measurements were made are available in Ref. [10].

Analysis was performed using a 1×3 unit cell with the a -axis along [001] ($A = 2.96 \text{ \AA}$) and the b -axis along [010] ($B = 13.77 \text{ \AA}$). The original diffraction pattern showed symmetry and systematic absences compatible with four possible plane groups: pm , pg , $p2mm$ and $p2mg$. The glide planes were taken along the [001] axis and mirror planes along the [010] axis. Phases for the structure factors were calculated using a minimum entropy Sayre-type equation with unitary structure factors and a robust figure of merit [17]. Using a genetic algorithm search method [15,25,26], phases were assigned and a FOM calculated based upon the self-consistency of the assigned phases. Because this is an imperfect case (i.e. a perfect data set would have zero errors and intensity measurement

Table 3

Relative titanium and oxygen atom positions of $\text{TiO}_{2-x}(100)\text{-}1 \times 3$ models with calculated χ^2 value

	Relative bulk TiO_{2-x} positions		4 Ti	4 Ti 2 Oxy	4 Ti 4 Oxy	4 Ti 3 Oxy	4 Ti 6 Oxy (b)	4 Ti 6 Oxy (a)	4 Ti 8 Oxy	4 Ti 7 Oxy	4 Ti 9 Oxy
	x pos	y pos ^a	x pos	x pos	x pos	x pos	x pos	x pos	x pos	x pos	x pos
	Ti 1	0.0	0.0	0.0	0.0	0.0	0.0	0.0	0.0	0.0	0.0
Ti 2	0.333	0.0	0.359	0.358	0.359	0.382	0.368	0.370	0.384	0.369	0.366
Ti 3	0.666	0.0	0.608	0.609	0.611	0.627	0.610	0.608	0.633	0.610	0.610
Ti 4	0.166	0.5	0.179	0.184	0.184	0.194	0.192	0.184	0.199	0.192	0.189
Ti 5	0.500	0.5									
Ti 6	0.833	0.5									
Oxy 1		0.0		0.145	0.149	0.069	0.171	0.075	0.076	0.061	0.015
Oxy 2		0.5		0.304	0.317	0.336	0.324	0.327	0.325	0.328	0.327
Oxy 3		0.0			0.585		0.515		0.586		0.587
Oxy 4		0.5			0.663		0.643		0.662		0.647
Oxy 5		0.5				0.952	0.937			0.917	0.938
Oxy 6		0.5					0.430	0.420	0.452	0.418	0.404
Oxy 7		0.5						0.037	0.043	0.029	0.049
Oxy 8		0.0						0.265	0.223	0.259	0.267
Oxy 9		0.0						0.923	0.894	0.948	0.918
χ^2			3.45	2.27	2.78	2.17	1.56	1.12	1.054	0.937	0.805
D.o.F.			15	13	11	13	9	9	7	9	7
%			0.002	0.5	0.1	0.8	12.2	34.7	39.6	49.8	40.8

^a For *pm* symmetry, atoms were refined only along the *x*-axis.

extending out to infinity), a low FOM will correspond to a plausible solution, but not necessarily the “true” solution. For each plane group, the best two or three unique solutions were examined. Charge density maps were generated, then used to construct surface structure models of the Ti atom positions. After the Ti atom positions were allowed to relax, a global *R*-factor was calculated comparing the model with the measured structure factors. The *R*-factor was of the form:

$$R = \frac{\sum_{\mathbf{h}} ||F_o(\mathbf{h})| - |F_c(\mathbf{h})||}{\sum_{\mathbf{h}} |F_o(\mathbf{h})|}$$

where F_o and F_c represent the observed (measured) and calculated structure factors for a given reflection \mathbf{h} summed over all reflections. These models provided initial estimates of the Ti atomic positions for χ^2 refinement. Only those models with reasonable *R*-factors were used to refine the final atomic positions.

The χ^2 used to refine the atomic positions and evaluate the model is of the form:

$$\chi^2 = \frac{1}{N-m} \sum_{\mathbf{h}} \frac{(|F_o(\mathbf{h})|^2 - |F_c(\mathbf{h})|^2)^2}{\sigma^2(\mathbf{h})}$$

where σ are the measured errors, N is the total number of reflections and m the number of parameters being fitted. For a perfect fit of the model to the observed structure factors within experimental uncertainty, χ^2 should be equal to 1. In certain cases, the value of the Ti Debye–Waller factor was included as a fitting parameter along with the atomic positions in the refinement. However, the value of the Debye–Waller did not contribute greatly to the χ^2 , and was limited to a range of 0.5 to 15 times the bulk Ti Debye–Waller value. One Ti atom was fixed to define the unit cell origin, and the remaining atoms were allowed to relax relative to it. Since titanium is the dominant scatterer in the unit cell, initially only the positions of the Ti atoms were refined. Once the best solutions

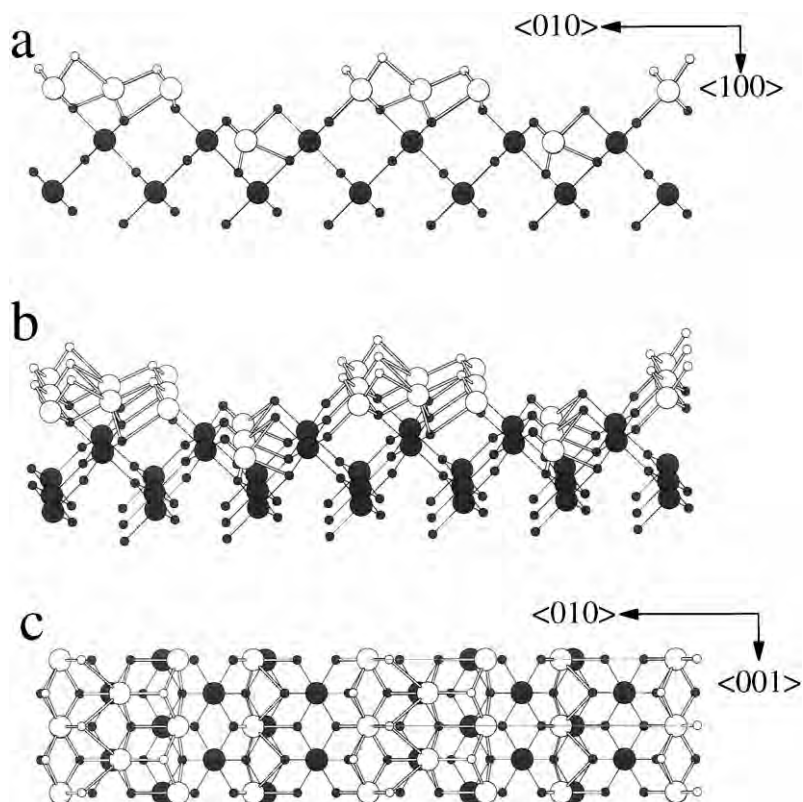


Fig. 4. Atomic model corresponding to 4 Ti 3 Oxy from Table 3 looking (a) along the $\langle 001 \rangle$, (b) tilted 10° off the $\langle 001 \rangle$, and (c) along the $\langle 100 \rangle$ directions. The larger circles represent titanium atoms and the smaller represent oxygen atoms. The open circles are the atoms whose positions have been refined through χ^2 minimization, and the filled circles correspond to bulk atomic positions.

were achieved, refinement of the oxygen atom positions was included.

The same set of data was also analyzed using maximum entropy (ME) methods [27]. These have a similar statistical basis to traditional direct methods, but employ more sophisticated statistics in the process of deriving phases. For a full description of the method when applied to surfaces, see Ref. [14]. All four plane groups were investigated, and in each case a 256 node, single level phasing tree was constructed [27]. Each node corresponds to a phase combination constructed from four strong reflections and each possible phase combination is subjected to entropy maximization. The calculations were fully automatic using the MICE computer program in default mode. Solutions from ME and direct methods were then compared as a crosscheck for additional possible solutions, and

for an independent assessment of the viability of the solutions that were chosen.

3. Results

Because the charge density around individual atoms can be approximated as being circular in projection, bright circular features in the generated charge density maps are normally interpreted as atom sites. However, with only 19 beams, all sampled from the same limited subquadrant of reciprocal space, the charge density for a single atom no longer appears as a well-defined disc due to the missing information. In addition, as more atoms are included in the unit cell, interference generates artifacts that can be mistaken as possible atom sites, see Fig. 1. Nonetheless, by comparing

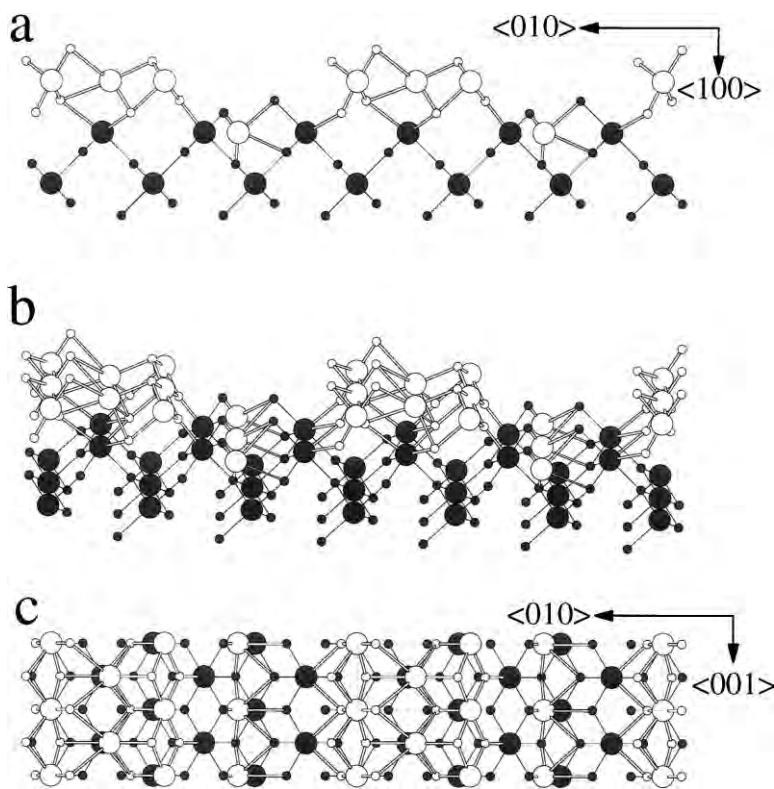


Fig. 5. Atomic model corresponding to 4 Ti 7 Oxy from Table 3 viewed (a) along the $\langle 001 \rangle$, (b) tilted 10° off the $\langle 001 \rangle$, and (c) along the $\langle 100 \rangle$ directions.

the charge density map of a single Ti atom using the same 19 reflections to the calculated charge density maps, one can obtain candidate Ti atom positions in the unit cell. Fig. 2 is an example of a charge density map generated from the direct phasing and its corresponding model constructed by placing a Ti atom (Fig. 1a) at each of the strong candidate sites.

From the initial set of solutions generated by the direct methods, after placing Ti atoms at the strong sites only three possible configurations gave reasonable fits to the data, one with four Ti atoms and two variants with five Ti atoms. (Only models with an R -factor corresponding to 0.41 or lower were included, any models with obvious differences between the measured and calculated structure factors were ignored. This excluded all the solutions investigated except those with pm plane group symmetry.) Table 2 summarizes both the refined positions and also provides a comparison with the

microfacet and missing row models previously considered [10]. The only solution that adequately explains the experimental data is the four Ti atom model shown in Fig. 2. Fig. 3b compares the measured structure factors and those corresponding to the model with four Ti atoms in the unit cell (Fig. 2) which has an R -factor of 0.26.

Just including the titanium atoms, and excluding possible oxygen sites is unreasonable – the χ^2 value at 3.45 is still high and the probability of finding such a value or higher using standard statistical tests is only 0.002%. Fortunately, the bulk solid-state chemistry of the non-stoichiometric oxide TiO_{2-x} is well established, involving edge- and corner-sharing octahedral units [28–30]. This provides chemical constraints which can be combined with the refinements. The results of including oxygen atoms at different octahedral sites are summarized in Table 3, and have a dramatic effect on the calculated χ^2 with good agreement between

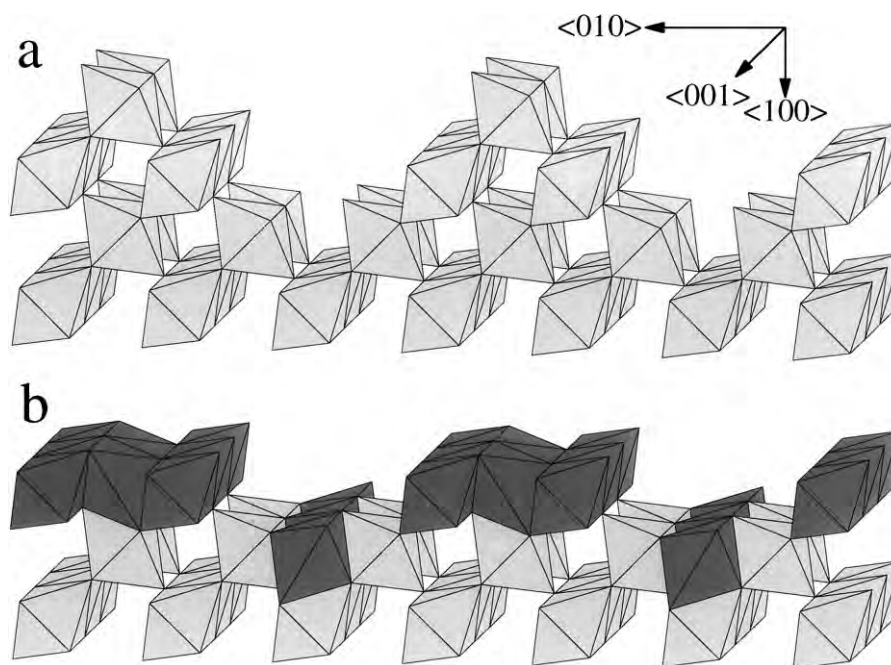


Fig. 6. Octahedra model schematic representation of (a) the microfacet model and (b) our proposed model. At the center of each octahedra is a titanium atom and oxygen atoms are positioned at the corners. The darker shade is used to highlight the major differences between (a) and (b).

experimental and calculated data for six to eight oxygen atoms. Fig. 4 is a model of the $\text{TiO}_{2-x}(100)-1 \times 3$ surface with four surface titanium and three surface oxygen atoms; Fig. 5 has four surface titanium atoms and seven oxygen while Fig. 6 is a more conventional octahedral representation. Because no rel-rod data normal to the surface is available, bulk atomic displacements perpendicular to the surface were used.

4. Discussion

Interpretation of the structure is relatively simple, particularly using the octahedral representation. Rather than only corner-sharing oxygen, edge-sharing sites are formed. Relative to only corner-sharing octahedra, there are two edge-sharing sites per unit cell leading to a nominal oxygen loss of three oxygen atoms. {Spectroscopic studies indicate the $\text{TiO}_{2-x}(100)$ surface reduces when annealed to produce the higher order reconstruction [4,7,9,11].} In the edge-sharing locations the

titanium atoms occupy octahedral sites, resembling the NaCl structure, unlike bulk rutile which occupies only half of the octahedral sites. This is a standard configuration for non-stoichiometric defects such as crystallographic shear planes in the bulk [28–30] and suggests that the surface can be considered as an ordering of similar defects at the surface. Extrapolating to a 1×5 and 1×7 periodicity would further reduce the oxygen content of the surface, which is also supported by the literature. Furthermore, it can be hypothesized that the 1×5 and 1×7 structures have the same occupancy of the surface octahedral sites as the 1×3 surface. In effect, there is a homologous series of oxygen deficient Ti_xO_y reconstructions analogous to the solid Magneli phases $\text{Ti}_n\text{O}_{2n-1}$ [28–30]. (Without definite information about the exact oxygen content we cannot be precise about the stoichiometry of the surface homologous series.)

As can be seen from Figs. 4 and 5 and Table 3, the positions of the Ti atoms remain consistent, regardless of the number of oxygen atoms included in the minimization. This is due to the relatively

weak scattering from the oxygen atoms compared to titanium. The oxygen atom positions, with the exception of Oxy 1 for model 4 Ti 9 Oxy, are also consistent for every model with the best fit for six to eight oxygen atoms. However, by adding more oxygen atoms to the refinement, the number of fitting parameters in the χ^2 increases, and the degrees of freedom decrease. This can cause χ^2 to reach a value less than one and also influence the confidence of the χ^2 value.

It is problematic to discuss a detailed analysis of the oxygen refinement with only 19 unique measured reflections. In addition, there may well be only partial occupancy of some of the outermost oxygen sites. Therefore the atomic positions given for the oxygen should not be considered better than the scatter among the different models, i.e. 0.2–0.3 Å. By comparison the titanium atom sites do not change much with oxygen content, so are probably accurate to 0.1 Å or better.

In addition to correlating well with the known bulk chemistry of TiO_{2-x} , it is worth mentioning that our model does share some of the same characteristics with those proposed by Oliver et al. [11], which were constructed using atomistic simulations and electronic considerations. In our model the top three Ti atoms lie at the same level, similar to the relaxed atom positions shown by Oliver et al. Previous studies using scanning tunneling microscopy [8,31,32] images of the $\text{TiO}_{2-x}(100)-1 \times 3$ surface are also consistent with our proposed model.

At the time the data set was collected, it represented the best that could be achieved with the apparatus [10,33,34]. Limits in the ability to search reciprocal space were a result of design constraints for the surface diffraction system. These same geometric constraints hampered the ability to measure along the reciprocal space rel-rods, limiting any structure information to within the plane of the surface. A more thorough exploration of reciprocal space and scans along the surface rel-rods of the $\text{TiO}_2(100)-1 \times 3$ surface would facilitate a more detailed analysis of the oxygen positions, possible oxygen vacancies, subsurface relaxations, and atomic position normal to the surface. Nonetheless, from the original GIXD data, along with the direct methods, it is evident

that a unit cell containing four titanium atoms and six to eight oxygen atoms provides the best solution for the $\text{TiO}_{2-x}(100)-1 \times 3$ surface.

Acknowledgements

We would like to acknowledge the support of the National Science Foundation via Grant #DMR-9214505 in funding this work. CJG wishes to acknowledge support from the EPSRC.

References

- [1] A. Fujishima, K. Honda, *Nature* 238 (1972) 37.
- [2] V.E. Henrich, *Progr. Surf. Sci.* 9 (1979) 143.
- [3] V.E. Henrich, G. Dresselhaus, H.J. Zeiger, *Solid State Commun.* 24 (1977) 623.
- [4] Y.W. Chung, W.J. Lo, G.A. Somorjai, *Surf. Sci.* 64 (1977) 588.
- [5] A. Szabo, T. Engel, *Surf. Sci.* 329 (1995) 241.
- [6] C.C. Kao, S.C. Tsai, M.K. Bahl, Y.W. Chung, *Surf. Sci.* 95 (1980) 1.
- [7] C.A. Muryn, P.J. Hardman, J.J. Crouch, G.N. Raiker, G. Thornton, *Surf. Sci.* 251/252 (1991) 747.
- [8] P.W. Murray, F.M. Leibsle, H.J. Fisher, C.F.J. Flipse, C.A. Muryn, G. Thornton, *Phys. Rev. B* 46 (1992) 12877.
- [9] C.C. Kao, S.C. Tsai, M.K. Bahl, Y.W. Chung, *Surf. Sci.* 95 (1980) 1.
- [10] P. Zschack, J.B. Cohen, Y.W. Chung, *Surf. Sci.* 262 (1992) 395.
- [11] P.M. Oliver, S.C. Parker, J. Purton, D.W. Bullett, *Surf. Sci.* 307–309 (1994) 1200.
- [12] S. Munnix, M. Schmeits, *Phys. Rev. B* 30 (1984) 2202.
- [13] M.M. Woolfson, *Acta Crystallogr.* A43 (1987) 593.
- [14] C.J. Gilmore, L.D. Marks, D. Grozea, C. Collazo, E. Landree, R.D. Twisten, *Surf. Sci.* 381 (1997) 77.
- [15] E. Landree, C. Collazo-Davila, L.D. Marks, *Acta. Crystallogr.* B53 (1997) 916.
- [16] L.D. Marks, R. Plass, D.L. Dorset, *Surf. Rev. Lett.* 4 (1997) 1.
- [17] L.D. Marks, E. Landree, *Acta Crystallogr. A*, in press.
- [18] C. Collazo-Davila, L.D. Marks, K. Nishii, Y. Tanishiro, *Surf. Rev. Lett.* 4 (1997) 65.
- [19] L.D. Marks, D. Grozea, R. Feidenhans'l, M. Nielsen, R.J. Johnson, *Surf. Rev. Lett.*, in press.
- [20] C. Collazo-Davila, D. Grozea, L.D. Marks, *Phys. Rev. Lett.* 80 (1998) 1678.
- [21] P.S. White, M.M. Woolfson, *Acta Crystallogr.* (1975) 53.
- [22] J.X. Yao, *Acta Crystallogr.* A37 (1981) 642.
- [23] C.J. Gilmore, W.V. Nicholson, *Trans. Am. Crystallogr. Assoc.* 30 (1994) 15.
- [24] D.E. Goldberg, *Genetic Algorithms in Search, Optimiza-*

- tion, and Machine Language, Addison-Wesley, Reading, MA, 1989.
- [25] Y.L. Xiao, D.E. Williams, Chem. Phys. Lett. 215 (1993) 17.
- [26] M.W. Gutowski, J. Phys. A: Math. Gen. 27 (1994) 7893.
- [27] G. Bricogne, G.J. Gilmore, Acta. Crystallogr. A46 (1990) 284.
- [28] C.N.R. Rao, J. Gopalakrishnan, New Directions in Solid State Chemistry, Cambridge University Press, Cambridge, 1997, pp. 257–277.
- [29] A.F. Wells, Structural Inorganic Chemistry, Oxford Science Publications, Oxford University Press, New York, 5th edn., 1991, pp. 562–565.
- [30] K. Kosuge, Chemistry of Non-Stoichiometric Compounds, Oxford University Press, Oxford, 1994, pp. 115–129.
- [31] P.W. Murray, F.M. Leibsle, C.A. Muryn, H.J. Fisher, C.F.J. Flipse, G. Thornton, Surf. Sci. 321 (1994) 217.
- [32] P.W. Murray, F.M. Leibsle, C.A. Muryn, H.J. Fisher, C.F.J. Flipse, G. Thornton, Phys. Rev. Lett. 72 (1994) 689.
- [33] P. Zschack, J.B. Cohen, Y.W. Chung, J. Appl. Cryst. 21 (1988) 466.
- [34] P. Zschack, Atomic structure of the $\text{TiO}_2(100)-(1 \times 3)$ surface determined with glancing angle X-ray diffraction and low energy electron diffraction, Ph.D. Dissertation, Northwestern University, Evanston, 1989.